

**Phase diagrams and multicritical points in randomly mixed magnets.
II. Ferromagnet-antiferromagnet alloys.**

Shmuel Fishman and Amnon Aharony

Department of Physics and Astronomy, Tel Aviv University, Ramat Aviv, Israel

(Received 5 July 1978)

The phase diagrams and critical behavior of a quenched random alloy of a ferromagnet and an antiferromagnet (or of two antiferromagnets with different periodicities) are studied in the mean-field approximation and by renormalization-group techniques. The antiferromagnetic order parameters are transformed into combinations of ferromagnetic order parameters, in order to study the possibility that ferromagnetic and antiferromagnetic orderings will become critical simultaneously. Averaging over the random variables yields a translationally invariant effective Hamiltonian, in which the m -component order parameters are replaced by nm -component order parameters and the limit $n \rightarrow 0$ is taken in the end of the calculation. The phase diagram in the concentration-temperature plane is obtained in the mean-field approximation, and the nature of the ordered phases is discussed. In addition to the ordered phases of the pure ingredients, a mixed phase is sometimes found. For $m > 1$, the ferromagnetic- and antiferromagnetic-order-parameter vectors are perpendicular to each other in this phase. The renormalization group is applied to study the multicritical point at which all these ordered phases meet. We don't find a stable fixed point appropriate for the description of this multicritical point. The physical implications of this fact are discussed. Finally, experiments on random alloys are reviewed and problems that should be studied experimentally are raised.

I. INTRODUCTION

Critical properties of quenched alloys have recently been the center of much interest.¹ In a recent paper,² we concentrated on the phase diagram and the critical properties of a quenched random alloy of two materials exhibiting *competing anisotropies*. In that case we treated an m -component classical spin system, where one ingredient of the mixture tends (when pure) to align only the first m_1 spin components while the other tends to align the remaining $m_2 (=m - m_1)$ components. The relative concentration of the components in the alloy, p , was the parameter determining the average spin anisotropy of the alloy and therefore determining which of the m spin components will order. The main result in I was the p - T (concentration-temperature) phase diagram depicted in Fig. 1(a). Phases I and II represent ordering of only m_1 or m_2 spin components. These phases are separated by a *mixed phase*, in which all m spin components are ordered. The diagram also exhibits a *tetracritical "decoupled" point*, at which each of the two order parameters undergoes its own phase transition even though both transitions occur simultaneously.

In this paper we study quenched alloys of materials which (when pure) exhibit ferromagnetic (FM) ordering with materials exhibiting antiferromagnetic (AFM) ordering. Although for definiteness we shall study FM-AFM mixtures, the analysis is also ap-

propriate for mixtures of antiferromagnets with different periodicities commensurate with the lattice periodicity. As in the previous case, the relative concentration of the components, p , is the parameter determining the type of ordering. Experience with other cases of competing interactions^{3,4} leads us to expect one of the phase diagrams shown in Fig. 1, where now I and II stand for FM and AFM. The present paper aims at checking these expectations.

Unlike the multicritical phase diagrams in anisotropic antiferromagnets,³ many experiments on random alloys exhibit a mixed phase.⁵⁻⁹ However, most of these experimental phase diagrams are incom-

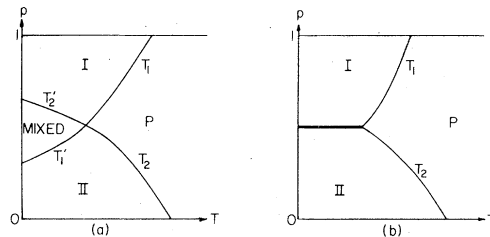


FIG. 1. Phase diagrams of random alloys. The ordered phases I and II are the same as in the pure materials (when $p = 1$ or 0). P denotes the paramagnetic phase. In case (a), the mixed phase has both I and II orderings simultaneously, and all the transitions are second order. In case (b), I and II are separated by a first-order line.

plete.⁵⁻¹³ Some of these alloys also have competing anisotropies, as discussed in I, and these should also be taken into account when the results of the present paper are applied to real systems. Many other alloys can be analyzed along the lines of the present paper.

In the problem of competing anisotropies, discussed in I, the competing order parameters consist of *different* m_1 and m_2 spin components. In the present problem, the competing order parameters correspond to FM and AFM orderings (or AFM orderings with different periodicities) and are thus obtained from *the same* spin components. This leads to additional terms in the effective Hamiltonian, which were not present in the Hamiltonian of the previous problem. These terms turn out to be relevant, leading to the instability of the "decoupled" fixed point that described the tetracritical point in the previous work. In fact, they lead to the absence of any physical stable fixed point appropriate for the description of the multicritical point in the phase diagrams of Fig. 1. Absence of stable fixed points is usually interpreted as leading to a first-order transition.¹⁴⁻¹⁵ However, in random systems the situation may be different.¹⁶ For instance, the transition may be smeared¹⁷ because different regions can undergo the transition at different temperatures. Other possibilities will be discussed below (Sec. V).

As in I, the randomness may be introduced either as bond randomness, where the coupling between the spins is a random variable, or as site randomness, where the identity of the magnetic ions on the various sites is random. These types of randomness are realized experimentally by mixing materials with identical magnetic ions but with different atoms mediating the superexchange^{5,9-13} (bond randomness) or by mixing materials with different magnetic ions⁶⁻⁸ (site randomness). In this work we study space-averaged order parameters (magnetization and staggered magnetization) and therefore our analysis is unable to predict how the specific types of ions order (i.e., in an alloy consisting of magnetic ions A and B we are unable to predict whether in a phase that orders on the average as pure A the ions B are also ordered similarly to the A ions). Since in this work we do not distinguish (for site randomness) between contributions of the different ions to the averaged magnetization, site randomness can be regarded as bond randomness with short-range correlations. These are unimportant for critical phenomena when long-range magnetic ordering occurs,¹⁸ so we shall confine ourselves to uncorrelated *bond randomness* in what follows. Throughout this paper we assume *long-range magnetic ordering*. For a random-bond alloy, spin-glass¹⁹ ordering is also possible. This possibility will be discussed in a forthcoming paper.²⁰ In some special cases of site randomness, absence of long-range magnetic order leads to a "spin glass" with critical properties identical to those of the long-range

orderings²¹ that will be analyzed in this paper.¹

The lack of translational invariance, which is the main difficulty in the treatment of random systems, is treated (as in I) by the " $n \rightarrow 0$ replica method."^{1,22,23} The difficulty in the treatment of possible simultaneous orderings with different periodicities is avoided using a generalization of a method introduced by Nelson and Fisher,³ in which all the order parameters are transformed to ferromagnetic ones by folding the Brillouin zone onto itself.

In Sec. II we derive a translationally invariant effective Hamiltonian by the above-mentioned methods. In Sec. III, mean-field theory is used to obtain the phase diagram. We show that the phase diagrams of Fig. 1 can indeed occur, and we summarize the mean-field criteria for which each of the possible phase diagrams is to be expected to give correctly the qualitative nature of the ordered phases. In order to study the critical region renormalization-group theory should be applied.²⁴⁻²⁶ At the lines T_1, T_2, T_1', T_2' of Fig. 1 only one order parameter becomes critical. Therefore, these transitions are identical to those of the appropriate one-component random systems, that were already studied.^{18,22,23,27,28} In Sec. IV, renormalization-group theory²⁴⁻²⁶ is used to study the critical behavior in the vicinity of the multicritical point of Fig. 1. We do not find a stable fixed point, leading to the conclusion that a usual second-order transition is impossible at this point. This is in contrast to mean-field theory. In Sec. V we discuss the physical consequences of the results and their relevance to experiments.

II. HAMILTONIAN

The Hamiltonian of our random spin system is

$$\mathcal{H} \{ [J_{ij}, \vec{S}(i)] \} = - \sum_{\langle ij \rangle} J_{ij} \vec{S}(i) \cdot \vec{S}(j) \quad , \quad (2.1)$$

where $\vec{S}(i)$ is an m -component spin vector at the site i of a d -dimensional lattice and J_{ij} is a random exchange coupling. As in I, we shall assume that each bond $\langle ij \rangle$ is independent of the others and is characterized by a distribution function $p(J_{ij})$. Site randomness (where J_{ij} depends on the identity of the ions occupying sites i and j) leads to an effective Hamiltonian of the same form.

We shall study the possibility of competing types of ordering (FM-AFM or AFM with different periodicities). Therefore, we have to introduce new order parameters corresponding to these orderings. We generalize a method introduced by Nelson and Fisher³ and applied to random systems by one of us.²⁹ Let us assume that we mix materials which (when pure) exhibit AFM structures commensurate with the lattice periodicity (in this section, a FM will be considered as a special case of an AFM with one spin per unit magnetic cell). The lattice is now divided into

cells, which are the minimal cells which include all the possible magnetic unit cells in the mixed magnets. This procedure is demonstrated in Fig. 2 for the two-dimensional square lattice. If each of these cells contains l spins, then there are l independent possible magnetic orderings. We now define cell spin variables,

$$\bar{\phi}_k(j) = \sum_{i=1}^l \bar{F}_{ki} \bar{S}(j,i), \quad k=1, \dots, l \quad (2.2)$$

where $\bar{S}(j,i)$ is the i th spin in the j th cell, k denotes the type of magnetic ordering, and the matrix \bar{F}_{ki} can be chosen to be orthonormal. $\bar{\phi}_k$ are the order parameters appropriate for the description of the various magnetic orderings. They are a generalization of the magnetization and the two sublattice staggered magnetization of Ref. 3. The old spin variables, expressed in terms of the new order parameters, are

$$\bar{S}(j,i) = \sum_{k=1}^l F_{ik} \bar{\phi}_k(j), \quad (2.3)$$

where $F_{ik} = \bar{F}_{ki}$. If $k=1$ denotes the FM, $F_{i1} = 1/\sqrt{l}$, and therefore

$$\sum_{i=1}^l \frac{F_{ik}}{\sqrt{l}} = \delta_{1k},$$

since due to orthonormality

$$\sum_i F_{ik} F_{ik'} = \delta_{kk'}.$$

For instance, for the magnets whose orderings are given in Fig. 2,

$$F = \frac{1}{\sqrt{4}} \begin{pmatrix} 1 & -1 & 1 & -1 \\ 1 & -1 & -1 & 1 \\ 1 & 1 & -1 & -1 \\ 1 & 1 & 1 & 1 \end{pmatrix}. \quad (2.4a)$$

Note that if we mix *one* of the AFM's whose orderings are depicted in Fig. 2(c) and 2(d) with the FM [Fig. 2(b)], then the minimal unit cell includes only two spins and F reduces to a 2×2 matrix,

$$\bar{W}(\bar{\phi}_k) = \frac{1}{2} \sum_{k=1}^l \bar{\phi}_k \cdot \bar{\phi}_k + \frac{v_0}{l} \left(\sum_{k=1}^l \bar{\phi}_k \cdot \bar{\phi}_k \bar{\phi}_k \cdot \bar{\phi}_k + \sum_{k'>k} (2 \bar{\phi}_k \cdot \bar{\phi}_k \bar{\phi}_{k'} \cdot \bar{\phi}_{k'} + 4 \bar{\phi}_k \cdot \bar{\phi}_{k'} \bar{\phi}_k \cdot \bar{\phi}_{k'}) \right) + \dots \quad (2.7)$$

The partition function is then transformed into

$$Z = \int \left(\prod_j \prod_{k=1}^l d\bar{\phi}_k(j) \right) e^{-\bar{W}(\bar{\phi}_k(j))} \times \exp(-H\{[J_{jj'}^{kk'}, \bar{\phi}_k(j)]\}/k_B T) \quad (2.8)$$

$$F = \frac{1}{\sqrt{2}} \begin{pmatrix} 1 & 1 \\ 1 & -1 \end{pmatrix}. \quad (2.4b)$$

The transformation [(2.2) and (2.3)] of \bar{S} into $\{\bar{\phi}_k\}_{k=1}^l$ leads to a reduction of the Brillouin zone by a factor l .³⁰ In most physical cases, $l=2^L$ (L integer) and all F_{ik} can be taken as $\pm 1/\sqrt{l}$. Therefore, this assumption will be made in what follows. In terms of the $\bar{\phi}_k$ variables, the Hamiltonian (2.1) is

$$\mathcal{H}\{[J_{jj'}^{kk'}, \bar{\phi}_k(j)]\} = -\frac{1}{2} \sum_{k,k'=1}^l \sum_{jj'} J_{jj'}^{kk'} \bar{\phi}_k(j) \cdot \bar{\phi}_{k'}(j'), \quad (2.5a)$$

where

$$J_{jj'}^{kk'} = \sum_{ii'} J_{ji,i'} F_{ik} F_{i'k'}. \quad (2.5b)$$

The transformations [(2.2) and (2.3)], transforming the Hamiltonian (2.1) into the form (2.5), can be performed for discrete as well as for continuous spins \bar{S} and $\bar{\phi}_k$. Let us assume that the spins are continuous, i.e., the Hamiltonian (2.1) was obtained from the real Hamiltonian by a Hubbard transformation.³¹ The resulting partition function is

$$Z = \text{Tr} \exp(-\mathcal{H}\{[J_{ij}, \bar{S}(i)]\}/k_B T) = \int \prod_i d\bar{S}(i) e^{-W(\bar{S}(i))} \times \exp(-\mathcal{H}\{[J_{ij}, \bar{S}(i)]\}/k_B T), \quad (2.6)$$

where k_B is the Boltzmann constant, T is the temperature and

$$W(\bar{S}) = \frac{1}{2} |\bar{S}|^2 + v_0 |\bar{S}|^4 + \dots$$

is the spin weight function.²⁶ The transformation transforming \bar{S} into $\{\bar{\phi}_k\}$ transforms $W(\bar{S})$ into

If \bar{S} and $\bar{\phi}_k$ are discrete spins, one should perform a Hubbard transformation³¹ on the Hamiltonian (2.5) in order to obtain continuous spins (required for renormalization-group studies²⁴⁻²⁶). This procedure, if performed, leads to the same partition function (2.8) that was obtained under the assumption that the spins \bar{S} are continuous.

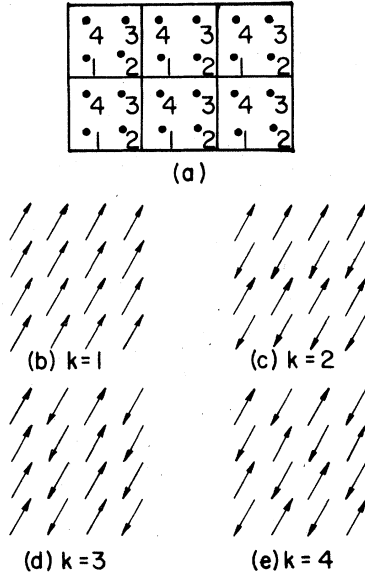


FIG. 2. Example of the construction of the magnetic order parameters for a square lattice. (a) The division of the lattice into cells. (b)–(e) The magnetic orderings appropriate for the order parameters $\vec{\phi}_k$, $k = 1, 2, 3, 4$.

In this example

$$\vec{\phi}_1(j) = 4^{-1/2} [\vec{S}(j, 1) + \vec{S}(j, 2) + \vec{S}(j, 3) + \vec{S}(j, 4)] ,$$

$$\vec{\phi}_2(j) = 4^{-1/2} [\vec{S}(j, 1) + \vec{S}(j, 2) - \vec{S}(j, 3) - \vec{S}(j, 4)] ,$$

$$\vec{\phi}_3(j) = 4^{-1/2} [\vec{S}(j, 1) - \vec{S}(j, 2) - \vec{S}(j, 3) + \vec{S}(j, 4)] ,$$

and

$$\vec{\phi}_4(j) = 4^{-1/2} [\vec{S}(j, 1) - \vec{S}(j, 2) + \vec{S}(j, 3) - \vec{S}(j, 4)]$$

[see Eq. (2.2)].

with

$$\begin{aligned} \mathcal{H}_{\text{eff}} = & \sum_{\alpha=1}^n \left[\frac{1}{2k_B T} \sum_{JJ'} \sum_{k=1}^l [J_{JJ'}^{kk}]_{\text{av}} \vec{\phi}_k^\alpha(j) \cdot \vec{\phi}_k^\alpha(j') - \sum_j \frac{1}{2} \sum_{k=1}^l \vec{\phi}_k^\alpha(j) \cdot \vec{\phi}_k^\alpha(j) \right. \\ & + \frac{v_0}{l} \sum_j \left[\sum_{k=1}^l \vec{\phi}_k^\alpha(j) \cdot \vec{\phi}_k^\alpha(j) \vec{\phi}_k^\alpha(j) \cdot \vec{\phi}_k^\alpha(j) + \sum_{k'>k} [2 \vec{\phi}_k^\alpha(j) \cdot \vec{\phi}_k^\alpha(j) \vec{\phi}_{k'}^\alpha(j) \cdot \vec{\phi}_{k'}^\alpha(j) + 4 \vec{\phi}_k^\alpha(j) \cdot \vec{\phi}_{k'}^\alpha(j) \vec{\phi}_k^\alpha(j) \cdot \vec{\phi}_{k'}^\alpha(j)] \right] \\ & + \frac{1}{(k_B T)^2} \sum_{JJ'} \sum_{\alpha, \beta=1}^n \left(\sum_{k=1}^l [(\Delta J_{JJ'}^{kk})^2]_{\text{av}} \vec{\phi}_k^\alpha(j) \cdot \vec{\phi}_k^\alpha(j') \vec{\phi}_k^\beta(j) \cdot \vec{\phi}_k^\beta(j') \right. \\ & + 2 \sum_{k'>k-1}^l \{ [\Delta J_{JJ'}^{kk} \Delta J_{JJ'}^{k'k'}]_{\text{av}} \vec{\phi}_k^\alpha(j) \cdot \vec{\phi}_k^\alpha(j') \vec{\phi}_{k'}^\beta(j) \cdot \vec{\phi}_{k'}^\beta(j') \\ & + [\Delta J_{JJ'}^{kk'} \Delta J_{JJ'}^{k'k}]_{\text{av}} \vec{\phi}_k^\alpha(j) \cdot \vec{\phi}_{k'}^\alpha(j') \vec{\phi}_k^\beta(j) \cdot \vec{\phi}_{k'}^\beta(j') \\ & \left. + [\Delta J_{JJ'}^{kk'} \Delta J_{JJ'}^{k'k}]_{\text{av}} \vec{\phi}_k^\alpha(j) \cdot \vec{\phi}_{k'}^\alpha(j') \vec{\phi}_k^\beta(j') \cdot \vec{\phi}_{k'}^\beta(j) \right) \left. \right] \dots \end{aligned} \quad (2.13)$$

The Hamiltonian (2.5) is not translationally invariant. One way to proceed is to transform (2.5) into a translationally invariant effective Hamiltonian, by averaging the free energy (the impurities are quenched!). As in I, instead of averaging the free energy $F = -k_B T \ln Z$ we replace $\ln Z$ by $(Z^n - 1)/n$ and take the limit $n \rightarrow 0$ at the end of the calculation.^{22,23} Considering Z^n amounts to replacing each of the m -component generalized spin vectors $\vec{\phi}_k$ by an nm -component vector $\{\vec{\phi}_k^1, \vec{\phi}_k^2, \dots, \vec{\phi}_k^n\}$, leading to

$$Z^n = \int \prod_J \prod_{\alpha=1}^n \prod_{k=1}^l d\vec{\phi}_k^\alpha(j) e^{\mathcal{H}_n} , \quad (2.9)$$

where

$$\begin{aligned} \mathcal{H}_n = & \sum_{\alpha=1}^n \left[\sum_{k', k=1}^l \frac{1}{2} \sum_{JJ'} \left(\frac{J_{JJ'}^{kk'}}{k_B T} \right) \right. \\ & \times \vec{\phi}_k^\alpha(j) \cdot \vec{\phi}_k^\alpha(j') \\ & \left. - \sum_j \bar{W} \{ \vec{\phi}_k^\alpha(j) \} \right] . \end{aligned} \quad (2.10)$$

We next decompose $J_{JJ'}^{kk'}$ as

$$J_{JJ'}^{kk'} = [J_{JJ'}^{kk'}]_{\text{av}} + \Delta J_{JJ'}^{kk'} , \quad (2.11)$$

where $[J_{JJ'}^{kk'}]_{\text{av}}$ is the configurational average of $J_{JJ'}^{kk'}$ and $J_{JJ'}^{kk'}$ can be decomposed in a similar way. As in I, we now expand the exponential of (2.9) in powers of $\Delta J_{JJ'}^{kk'}$, average over configurations and then exponentiate again. Finally, using the choices $l = 2^L$, $F_{ik} = \pm 1/\sqrt{l}$, we obtain

$$[Z^n]_{\text{av}} = \int \prod_J \prod_{k=1}^l \prod_{\alpha=1}^n d\vec{\phi}_k^\alpha e^{\mathcal{H}_{\text{eff}}} \quad (2.12)$$

where the dots represent higher-order terms. Since \mathcal{H}_{eff} satisfies the symmetry of the lattice, only even power of each $\vec{\phi}_k^\alpha$ appear. In particular, $\vec{\phi}_k^\alpha \cdot \vec{\phi}_{k'}^\alpha$ terms with $k \neq k'$ are absent. In the derivation of (2.13) we relied on the assumption that bonds are uncorrelated, leading to the conclusion that $[\Delta J_{j_1 j_2}^{k_1 k_2} \Delta J_{j_3 j_4}^{k_3 k_4}]_{\text{av}} \neq 0$ only if

$$\langle j_1 j_2 \rangle = \langle j_3 j_4 \rangle.$$

We now follow the usual renormalization-group routine²⁴⁻²⁶: we Fourier transform $\vec{\phi}_k^\alpha$, rewrite (2.13) as an expansion in powers of the components of $\vec{\phi}_k^\alpha(\vec{q})$, expand the coefficients in powers of the momenta \vec{q} , and rescale the spins $\vec{\phi}_k^\alpha(\vec{q})$, to obtain

$$\begin{aligned} \mathcal{H}_{\text{eff}} = & -\frac{1}{2} \int_{\vec{q}} \sum_{\alpha=1}^n \sum_{k=1}^l (r_k + q^2) \vec{\phi}_k^\alpha(\vec{q}) \cdot \vec{\phi}_k^\alpha(-\vec{q}) \\ & - \int_{\vec{q}_1} \int_{\vec{q}_2} \int_{\vec{q}_3} \sum_{\alpha, \beta=1}^n \sum_{k, k'=1}^l (u_{kk'} + v_{kk'} \delta_{\alpha\beta}) \vec{\phi}_k^\alpha(\vec{q}_1) \cdot \vec{\phi}_k^\alpha(\vec{q}_2) \vec{\phi}_k^\beta(\vec{q}_3) \cdot \vec{\phi}_{k'}^\beta(-\vec{q}_1 - \vec{q}_2 - \vec{q}_3) \\ & + \sum_{k \neq k'=1}^l (w_{kk'} + \bar{v}_{kk'} \delta_{\alpha\beta}) \vec{\phi}_k^\alpha(\vec{q}_1) \cdot \vec{\phi}_k^\alpha(\vec{q}_2) \vec{\phi}_k^\beta(\vec{q}_3) \cdot \vec{\phi}_{k'}^\beta(-\vec{q}_1 - \vec{q}_2 - \vec{q}_3) + \dots \end{aligned} \quad (2.14)$$

The integrals are over the range $|\vec{q}| < \Lambda$, where Λ is a typical size of the reduced Brillouin zone, $v_{kk'}$ and $\bar{v}_{kk'}$ are proportional to v_0/l and are positive, and

$$r_k = A_k [k_B T - \hat{J}^{kk}(0)] \quad (2.15)$$

Here, $\hat{J}^{kk}(\vec{q})$ is the Fourier transform of $[J_{jj'}^{kk}]_{\text{av}}$, and therefore

$$\hat{J}^{kk}(0) = \sum_{j, j'} [J_{j, j'}^{kk}]_{\text{av}} F_{jk} F_{j'k} \quad (2.16)$$

The other potentials in (2.14) are

$$u_{kk} = -B_1^{kk} \sum_{j, j'} \frac{[\Delta J_{j, j'}^2]_{\text{av}}}{l} \quad (2.17a)$$

$$u_{kk'} = -B_2^{kk'} \sum_{j, j'} [\Delta J_{j, j'}^2]_{\text{av}} F_{jk} F_{j'k'} F_{jk'} F_{j'k} \quad (2.17b)$$

$$\begin{aligned} w_{kk'} &= -B_3^{kk'} \sum_{j'} [(\Delta J_{j, j'}^{kk} + \Delta J_{j, j'}^{k'k})^2]_{\text{av}} \\ &= -B_3^{kk'} \sum_{j, j'} [\Delta J_{j, j'}^2]_{\text{av}} (F_{jk} F_{j'k'} + F_{jk'} F_{j'k})^2 \end{aligned} \quad (2.17c)$$

where A_k and $B_k^{kk'}$ are positive functions of temperature and concentration. These functions vary smoothly in the critical region, and therefore their explicit form is unimportant. Note that u_{kk} and $w_{kk'}$ are negative. The r_k 's are functions of temperature and concentration. For each concentration, the $\vec{\phi}_k^\alpha$ for which r_k is the smallest will order at the highest

temperature. In what follows we shall confine ourselves to a section of the phase diagram where $r_{k_1} \approx r_{k_2}$ and where these are much smaller than the rest of the r_k 's. Therefore, we integrate out all the $\vec{\phi}_k^\alpha$ except $\vec{\phi}_{k_1}^\alpha$ and $\vec{\phi}_{k_2}^\alpha$, and denote for simplicity $k_1 = 1$ and $k_2 = 2$. $\vec{\phi}_1^\alpha$ and $\vec{\phi}_2^\alpha$ may be FM and AFM order parameters or two different AFM order parameters. In what follows we confine ourselves, for definiteness, to the case when $\vec{\phi}_1$ and $\vec{\phi}_2$ correspond to FM and AFM orderings, respectively. The analysis for the competition of two different AFM orderings is identical. The Hamiltonian (2.14) would be identical to the Hamiltonian (2.10) of I if the last term in (2.14) were absent, i.e., if $w_{12} = \bar{v}_{12} = 0$. For $m = 1$ (Ising model), \bar{v}_{12} can be absorbed in v_{12} , and this term is absent if w_{12} vanishes. If $w_{12} = 0$, we see from (2.17c) that $F_{i1} F_{i2} = -F_{i2} F_{i1}$ for every i and i' . Since $F_{ik} = \pm 1/\sqrt{l}$, we find $F_{i1} F_{i1} = -F_{i2} F_{i2}$, yielding [by (2.16)] $\hat{J}^{11}(0) = -\hat{J}^{22}(0)$. Therefore, if $\vec{\phi}_1$ and $\vec{\phi}_2$ order simultaneously at a positive temperature, we must have $w_{12} \neq 0$ and \mathcal{H}_{eff} cannot reduce to the Hamiltonian of I.

The Hamiltonian (2.14) with $u_{kk'} = 0$ and $w_{kk'} = 0$ is a *pure system* Hamiltonian, which was already studied (when $r_1 = r_2$) by Brazovskii *et al.*¹⁵ in a different context. Mean-field theory predicts a second-order transition for this Hamiltonian, but renormalization-group studies predict the transition to become first order. Had we had pure systems which were described by the above-mentioned Hamiltonian, such that it would be experimentally possible to control $r_1 - r_2$ (e.g., by pressure), we would obtain phase diagrams of the type depicted in Fig. 1 (with p representing pressure), with second-order transitions

at the lines T_1, T_2, T_1', T_2' , and with a first-order transition at the multicritical point. For a simpler Hamiltonian, which yields the phase diagram of Fig. 1(b), Domany *et al.*³² recently found that the transitions along sections of the lines T_1 and T_2 close to the bicritical point may also become first order due to fluctuations. Analysis of the same Hamiltonian in the parameter range which yields Fig. 1(a) shows³³ that the first-order transition from the paramagnetic into the mixed phase may extend over a finite range of values of the parameter p . The lines T_1 and T_2 then end at critical end points on this first-order line. The same calculations have to be performed for our problems before we can make definite predictions on the final phase diagram in our case.

If impurities are mixed into a system which is described by the pure version of the Hamiltonian (2.14) ($u_{kk'}=0, w_{kk'}=0$), then the resulting random system will be described by the effective Hamiltonian (2.14). Therefore, our calculations are relevant also to that problem. If the randomness is weak, the Hamiltonian flows may be approximately close to those of the pure system studied in Ref. 15, leading to a first-order transition.

III. MEAN-FIELD THEORY AND PHASE DIAGRAMS

The mean-field (MF) approximation will be introduced by ignoring the spatial dependence of the order parameters, reflected by the term q^2 in (2.14) and by the replacements $\vec{\phi}_1^\alpha \rightarrow \vec{M}, \vec{\phi}_2^\alpha \rightarrow \vec{N}$, which are the FM and AFM order parameters, respectively. The order parameter is taken to be identical in all the replicas in order to preserve the replicated nature of the Hamiltonian (2.14) in the MF approximation. The resulting free energy per degree of freedom is (in the limit $n \rightarrow 0$)

$$\begin{aligned} \bar{F} &\equiv \lim_{n \rightarrow 0} (F/nk_B T) \\ &= \frac{1}{2}(r_1 M^2 + r_2 N^2) + v_{11} M^4 + v_{22} N^4 \\ &\quad + 2v_{12} M^2 N^2 + 4\bar{v}_{12} M^2 N^2 \cos^2 \theta, \end{aligned} \quad (3.1)$$

where $M = |\vec{M}|, N = |\vec{N}|, v_{11}, v_{22}, v_{12}$, and \bar{v}_{12} are positive, and $\cos \theta = \vec{M} \cdot \vec{N} / MN$. For $m=1, \theta$ is meaningless and \bar{v}_{12} can be absorbed in v_{12} . Note that $u_{kk'}$ and w_{12} drop out from the expression for F/n in the limit $n \rightarrow 0$, since they are multiplied by a factor n . We now have to find the values of N, M , and θ minimizing the free energy, as required in the MF approximation. It is obvious that at the minimum of $\bar{F}, \theta = \frac{1}{2}\pi$, and $\vec{M} \perp \vec{N}$ for $m > 1$. This result could be heuristically expected, because in MF theory the magnetization \vec{M} is equivalent to an effective uniform magnetic field acting on the AFM order parameter \vec{N} . An AFM in a uniform magnetic

field orders perpendicular to the field,³ hence we expect \vec{N} to order perpendicular to \vec{M} in the mixed phase.

Minimizing \bar{F} with respect to M and N when $\theta = \frac{1}{2}\pi$ we now find the four usual solutions,^{3,4,34} i.e., the paramagnetic phase ($M=N=0$), occurring for $r_1, r_2 > 0$, the FM phase ($N=0, M^2 = -r_1/4v_{11}$) occurring for $r_2 > 0, r_1 < 0$, the AFM phase ($M=0, N^2 = -r_2/4v_{22}$) occurring for $r_2 < 0, r_1 > 0$, and the "mixed" phase

$$\begin{aligned} M^2 &= -\frac{1}{4}(v_{22}r_1 - v_{12}r_2)/(v_{11}v_{22} - v_{12}^2), \\ N^2 &= -\frac{1}{4}(v_{11}r_2 - v_{12}r_1)/(v_{11}v_{22} - v_{12}^2). \end{aligned} \quad (3.2)$$

The "mixed" phase separates the FM and the AFM ones only if $v_{11}v_{22} > v_{12}^2$,³⁴ when Fig. 1(a) results. If $v_{11}v_{22} \leq v_{12}^2$, the phase diagram is as in Fig. 1(b). The multicritical point [tetracritical in Fig. 1(a) and bicritical in Fig. 1(b)] occurs at $r_1 = r_2 = 0$.

If the exact Hamiltonian consisted only of terms up to quartic order in the spins, then one can see from (2.7) that $v_{11} = v_{22} = v_{12} = v_0/l$ and $v_{11}v_{22} = v_{12}^2$. Since, in practice, higher-order terms are present, including powers of $\vec{\phi}_1^\alpha \cdot \vec{\phi}_2^\alpha$ that break the rotational symmetry in the $(\vec{\phi}_1^\alpha, \vec{\phi}_2^\alpha)$ space, the potentials $v_{kk'}$ differ from v_0/l due to contributions obtained when the noncritical degrees of freedom are integrated out and both inequalities between $v_{11}v_{22}$ and v_{12}^2 are possible.

In this section we minimized the free energy after the limit $n \rightarrow 0$ was taken. One can perform the operations of minimization and taking the $n \rightarrow 0$ limit in the alternative order, and the results remain unchanged. In some other cases, including spin glasses, the order of these steps may be important. We shall discuss these problems in a forthcoming paper.²⁰

Mean-field theory shows that the alloy will indeed exhibit one of the phase diagrams depicted in Fig. 1, and determines the nature of the ordered phases. In order to study the critical regions of the phase diagram one should apply the renormalization group. We divide our discussion of the renormalization-group analysis into two parts. In the first part, following below, we summarize known results concerning the transitions at the lines T_1, T_2, T_1' , and T_2' in Fig. 1. The second part, in Sec. IV, will concentrate on the vicinity of the multicritical point, where $r_1 \simeq r_2$. The lines T_1 and T_2 in Fig. 1 represent second-order transitions from the paramagnetic to the FM and AFM ordered phases, respectively. These transitions are described by the exponents of an m -component random magnet.^{18,22,27} It turns out that for $m > 1, d=3$, these exponents are identical to those of the corresponding pure magnet,^{18,22,28} whereas for $m=1$ (Ising model) one finds a different random behavior.^{27,28} For $m=1, T_1' (T_2')$ is the criti-

cal line at which $\vec{M}(\vec{N})$ orders. Therefore, the critical exponents are the same as for a random Ising magnet.²⁷ For $m > 1$, at T_1' (T_2') only $m - 1$ components of $\vec{M}(\vec{N})$ become critical, since in the mixed phase $\vec{M} \perp \vec{N}$. Therefore, the critical behavior along T_1' (T_2') is that of an $(m - 1)$ -component random magnet.^{18, 22, 27}

The multicritical point in Fig. 1 is determined by the condition

$$\hat{j}^{11}(0) = \hat{j}^{22}(0), \quad (3.3)$$

obtained from (2.15). If $\bar{\phi}_1^\alpha$ and $\bar{\phi}_2^\alpha$ are FM and AFM order parameters, respectively, and if J_{ij} of (2.1) includes only nearest-neighbor interactions, then (3.3) implies that the multicritical point of Fig. 1 occurs at $T = 0$. To see this, note that for the nearest-neighbor AFM, $F_{12}F_{1'2}$ in (2.16) is equal to $-1/l$ if $[J_{ijj'}]_{av} \neq 0$, whereas for the ferromagnet $F_{11}F_{1'1} = 1/l$. Therefore $\hat{j}^{11}(0) = -\hat{j}^{22}(0)$, and by (3.3) $\hat{j}^{11}(0) = \hat{j}^{22}(0) = 0$. It follows that in order to obtain

the above-mentioned multicritical point at a finite temperature it is necessary to assume at least additional *next-nearest-neighbor* interactions in the FM-AFM alloy, as will be done throughout this paper. This requirement is not always necessary if the competing order parameters are AFM with different periodicities.

IV. RENORMALIZATION-GROUP ANALYSIS OF THE MULTICRITICAL POINT

In this section we study the multicritical point of Fig. 1, by application of the renormalization group²⁴⁻²⁶ to the Hamiltonian (2.14) in the region where only $\bar{\phi}_1^\alpha$ and $\bar{\phi}_2^\alpha$ are critical. In the iteration process, we integrate over spins $\bar{\phi}_k^\alpha(\vec{q})$ with $\Lambda/b < |\vec{q}| < \Lambda$, and rescale all momenta by $\vec{q} \rightarrow b\vec{q}$ and all spins by $\bar{\phi}_k^\alpha(\vec{q}) \rightarrow \bar{\phi}_k^\alpha(b\vec{q}) = \zeta_k \bar{\phi}_k^\alpha(\vec{q})$, with $\zeta_k^2 = b^{d+2-\eta_k}$. To order $\epsilon = 4 - d$ the resulting recursion relations for the quartic spin terms are^{26, 35}

$$u_{11}' = b^\epsilon \{ u_{11} - 4K_4 \ln b [(8 + nm) u_{11}^2 + 2(m + 2) u_{11} v_{11} + 2m v_{12} u_{12} + nm u_{12}^2 + 4w_{12}^2 + 4u_{12} w_{12} + 4u_{12} \bar{v}_{12}] \}, \quad (4.1a)$$

$$v_{11}' = b^\epsilon \{ v_{11} - 4K_4 \ln b [(m + 8) v_{11}^2 + 12u_{11} v_{11} + 4w_{12} v_{12} + 8w_{12} \bar{v}_{12} + m v_{12}^2 + 4v_{12} \bar{v}_{12} + 4\bar{v}_{12}^2] \}, \quad (4.1b)$$

$$u_{12}' = b^\epsilon \{ u_{12} - 4K_4 \ln b [u_{12} [4u_{12} + (2 + nm)(u_{11} + u_{22}) + (2 + m)(v_{11} + v_{22})] + (m v_{12} + 2\bar{v}_{12} + 2w_{12})(u_{11} + u_{22}) + 4w_{12}^2] \}, \quad (4.1c)$$

$$v_{12}' = b^\epsilon \{ v_{12} - 4K_4 \ln b [v_{12} [4v_{12} + 8u_{12} + (2 + m)(v_{11} + v_{22}) + 2(u_{11} + u_{22})] + \bar{v}_{12} [4\bar{v}_{12} + 8w_{12} + 2(v_{11} + v_{22})] + 2w_{12}(v_{11} + v_{22})] \}, \quad (4.1d)$$

$$\bar{v}_{12}' = b^\epsilon \{ \bar{v}_{12} - 4K_4 \ln b [\bar{v}_{12} [(4 + 2m)\bar{v}_{12} + 8v_{12} + 8u_{12} + 4w_{12} + 2(u_{11} + u_{22}) + 2(v_{11} + v_{22})] + 2w_{12}(v_{11} + v_{22} + 2v_{12})] \}, \quad (4.1e)$$

$$w_{12}' = b^\epsilon \{ w_{12} - 4K_4 \ln b w_{12} [(4 + 2nm)w_{12} + 4(m + 1)\bar{v}_{12} + 4v_{12} + 8u_{12} + 2(u_{11} + u_{22})] \}, \quad (4.1f)$$

where

$$K_d^{-1} = 2^{d-1} \pi^{d/2} \Gamma(\frac{1}{2}d).$$

The recursion relations for u_{22} and v_{22} can be obtained from (4.1a) and (4.1b) by interchanging indices 1 and 2.

For $m = 1$, v_{12} and \bar{v}_{12} are both coefficients of the same operator in the Hamiltonian (2.14), and therefore \bar{v}_{12} can be absorbed in v_{12} by the replacement $2\bar{v}_{12} + v_{12} \rightarrow v_{12}$. The resulting recursion relations are identical to (4.1a)–(4.1f) except that \bar{v}_{12} should be eliminated and (4.1d) and (4.1e) should be replaced by

$$v_{12}' = b^\epsilon \{ v_{12}' - 4K_4 \ln b [v_{12}' [4v_{12}' + 8u_{12} + 2(u_{11} + u_{22}) + 3(v_{11} + v_{22})] + w_{12}' [8v_{12}' + 6(v_{11} + v_{22})] \}. \quad (4.1g)$$

If $w_{12}=0$, and $\bar{v}_{12}=0$ for $m > 1$, then the Hamiltonian (2.14) and its related recursion relations (4.1a)–(4.1g) reduce exactly to those of I. From (4.1) we see that for $w_{12}=\bar{v}_{12}=0$, Eqs. (4.1e) and (4.1f) decouple from the remaining recursion relations, and the fixed points of the Hamiltonian coincide with those of I. In I we found many fixed points, but only one of them turned out to be physical and stable. This stable physical fixed point was decoupled, i.e., $u_{12}^* = v_{12}^* = 0$, and corresponded to two independent "pure" m -component fixed points,

$$u_{11}^* = u_{22}^* = 0, \quad v_{11}^* = v_{22}^* = \epsilon/4K_4(m+8) + O(\epsilon^2), \quad (4.2a)$$

if $m > 1$, and to two independent Khmel'nitzkii "random" fixed points²⁷

$$u_{11}^* = u_{22}^* = -(3\epsilon/106)^{1/2}/4K_4 + O(\epsilon), \quad (4.2b)$$

$$v_{11}^* = v_{22}^* = (3\epsilon/106)^{1/2}/3K_4 + O(\epsilon),$$

if $m = 1$. In addition to the decoupled fixed point, another stable fixed point was found, i.e., the "isotropic $n = 0$ " fixed point, with

$$u_{11}^* = u_{22}^* = u_{12}^* = \epsilon/32K_4 + O(\epsilon^2), \quad (4.3)$$

$$v_{11}^* = v_{22}^* = v_{12}^* = 0.$$

However, this fixed point is unphysical, since it has positive u_{11}^* and u_{22}^* (Refs. 18, 22, 29) [see (2.17a)].

A simple linearization of the recursion relations [(4.1e)–(4.1g)] around the decoupled fixed point shows that this point is *unstable* against nonzero \bar{v}_{12} and w_{12} . The isotropic fixed point is stable, but probably irrelevant as mentioned above.

The stability of the decoupled fixed points against w_{12} near $w_{12}^* = 0$ can be examined by scaling considerations, independent of ϵ expansions.^{26,36} At a "pure" decoupled fixed point $u_{11}^* = u_{22}^* = u_{12}^* = 0$, w_{12} is a coefficient of a product of four independent spin operators $\bar{\phi}_k^\alpha$. Each spin operator scales as a magnetization, hence it behaves as $\xi^{-\beta_m/v_m}$ where β_m and v_m are the magnetization and correlation length exponents of the m -component model. The stability exponent against w_{12} is therefore

$$\lambda_w = d - 4\beta_m/v_m = 4 - d - 2\eta_m. \quad (4.4)$$

For $m > 1$, the "pure" fixed point is the only physical stable fixed point when $\bar{v}_{12}^* = 0$, $w_{12}^* = 0$. From (4.4), $\lambda_w > 0$ for $d < 4$ and therefore this fixed point is unstable against w_{12} . One should solve (4.1a)–(4.1f) for other possible fixed points to find the appropriate critical properties.

For the "random" or "Khmel'nitzkii" [see (3.5) of I] decoupled fixed points, w_{12} multiplies a product of

two independent spin anisotropy operators $\phi_{k,J}^\alpha \phi_{l,i}^\beta$ ($\phi_{k,J}^\alpha$ are the components of $\bar{\phi}_k^\alpha$). Each of these behaves as $\xi^{-(d-\phi_{nm}/v_{nm})}$, where ϕ_{nm} and v_{nm} are the exponents of the $g\bar{\phi}^\alpha \cdot \bar{\phi}^\alpha$ anisotropy crossover³⁷ and correlation length of the nm -component spin cubic Hamiltonian³⁸ (ϕ_{nm} corresponds to ϕ_3 of Ref. 38). The exponents ϕ_{nm} and v_{nm} can be obtained to leading order in ϵ (unfortunately they are unknown from other sources) from the recursion relations for r_1 and r_2 [(Eq. (3.1) of I]. The exponent of stability against w_{12} is

$$\lambda_w = d - 2(d - \phi_{nm}/v_{nm}) = 2\phi_{nm}/v_{nm} - d = \epsilon - 4u_{11}^*. \quad (4.5)$$

This is identical to the value obtained directly from (4.1f). We find $\lambda_w > 0$, since at physical fixed points $u_{11}^* < 0$. For $m = 1$ and $w_{12}^* = 0$ the decoupled "Khmel'nitzkii" fixed point is the only physical stable fixed point. Since it is unstable against w_{12} , one should again solve the recursion relations for all other possible fixed points.

Solution of the recursion relations (4.1) is intractable analytically except in the cases discussed above (see I). Therefore, we solved them numerically by the method presented in Appendix B of I. For $m = 1$, we solved (4.1a)–(4.1c), (4.1f), and (4.1g) for fixed points with $w_{12}^* \neq 0$. These lead to a system of six quadratic and one linear coupled equations, having at most $2^6 = 64$ solutions. We find 22 complex solutions, 23 real finite solutions, three of which have triple multiplicities, and 13 solutions which "run-away" to infinity. The connection between run-away solutions and solutions of order $\sqrt{\epsilon}$ was pointed out in Appendix B of I. The method outlined there enabled us to find the connection between the run-away solutions and the corresponding $\sqrt{\epsilon}$ solutions. We find that all except two run-away solutions correspond to the $\sqrt{\epsilon}$ solutions. In order to check the stability of an order $\sqrt{\epsilon}$ fixed point one does not need the actual values of the fixed point potentials v_{kk}^* , u_{kk}^* , w_{12}^* , \bar{v}_{12}^* , but only the ratios among them. Therefore, one does not have to calculate higher-order diagrams in order to check stability of these fixed points. We find that for $m = 1$ all the fixed points (of order ϵ and $\sqrt{\epsilon}$) are unstable, except for the unphysical "isotropic $n = 0$ " fixed point (4.3).

In order to solve numerically the fixed-point equations obtained from (4.1a)–(4.1f) for $m > 1$ we had to confine ourselves to a specific value of m . To the first order in ϵ , the "pure" fixed point (4.2a) is stable only for $m > 4$. However, we know from higher-order calculations and scaling considerations²⁶ that at $\epsilon = 1$ it is stable for all $m \geq 2$, and therefore describes the phase transition along T_1 of Fig. 1. In order to avoid artificial instabilities, which we know to exist only because of the low order of the ϵ expansion, we

solved (4.1a)–(4.1f) for fixed points with $m = 5$. Since we are interested only in qualitative behavior, the actual value of m chosen is unimportant, as long as we identify correctly the fixed point which describes the transition. The fixed point equations for $m > 1$ obtained from (4.1) have at most $2^8 = 256$ solutions. Sixty-four of these, for which $\bar{v}_{12}^* = w_{12}^* = 0$, were discussed above (again, the fixed points $v_{12}^* \neq 0$, $u_{12}^* \neq 0$, $\bar{v}_{12}^* = 0$, $w_{12}^* = 0$ are unstable). The remaining 192 solutions were found numerically. Of these, 124 are complex solutions and 58 are real solutions. Five of the real solutions are of triple multiplicity. Again, none of the fixed points except the unphysical "isotropic $n = 0$ " fixed point (4.3) is stable.

We conclude that *there is no stable physical fixed point that describes the multicritical point* in Fig. 1. Therefore the transition there is not a usual second-order one. The discussion about the possible nature of this transition is deferred to Sec. V.

V. CONCLUSIONS AND DISCUSSION

The main result of our renormalization-group analysis is the absence of a stable physical fixed point to describe the multicritical point. Although such a multicritical point, with a second-order transition, is predicted by mean-field theory, its nature is changed due to critical fluctuations. It is impossible to predict the explicit new nature of the phase transition at the multicritical point without further calculations. For example, one should iterate the recursion relations into a region in which the fluctuations are negligible, and then use mean-field theory to analyze the resulting effective Hamiltonian.^{15,32} Such an analysis is quite complicated for random systems,^{16,17} particularly because of difficulties with the replica method deep in the ordered phase.³⁹ Instead of performing such a complete analysis, we list here a few of the possible results.

(i) *The transition is first order.* As we noted following Eq. (2.13), our Hamiltonian reduces to that of a pure complex antiferromagnet when $u_{kk'} \approx w_{kk'} \approx 0$, i.e., when the second cumulants of the exchange coefficients are very small. The appropriate "pure" Hamiltonian was analyzed in Ref. 15, for $m > 1$. It was shown there, that the critical fluctuations turn the transition first order. Thus, if one somehow constructs a system with the two order parameters $\bar{\phi}_1$ and $\bar{\phi}_2$ almost degenerate but with small random fluctuations in the coupling constants, then the transition at the multicritical point will be first order. It may probably be expected that the same will remain true if $u_{kk'}$ and $w_{kk'}$ are relatively small [compared to v_0 , Eq. (2.13)], since they will not grow too large even at the stage when mean-field theory is used. The first-order transition is not expected for $m = 1$,¹⁵ so something else may be needed for describing the Ising

case.

If, indeed, the transition at the multicritical point becomes first order, then one may expect some ranges of first-order transitions along the lines T_1 and T_2 as well, ending at tricritical points.³² An alternative possibility is a first-order transition from the paramagnetic into the mixed phase, extending over a finite range of values of p .³³ The critical lines T_1 and T_2 then end at critical end points at this first-order line. However, only explicit calculations, similar to those of Refs. 32 and 33 can give details.

(ii) *The transition is smeared.* The effect of randomness on Hamiltonians of the type discussed in Refs. 14 and 15 was studied by Bak.¹⁷ Following his arguments, one should iterate the renormalization group until critical fluctuations are eliminated. At that stage, the parameters $u_{kk'}$ and $w_{kk'}$ which represent variances in the exchange coefficients may become quite large. Assuming (as we have been) short-range correlations among the impurities, we end up with different domains of the system which undergo the first-order transition discussed above at different transition temperatures, with a wide range of such temperatures. The superposition of all these transitions appears as a smeared transition.^{18,36} The extent of smearing will depend on the initial values of $u_{kk'}$ and $w_{kk'}$, i.e., on the amount of randomness.

(iii) *The transition is eliminated or turned first order.* As noted in Sec. II, the "random" Hamiltonian (2.5) includes terms like $J_{jj'}^2 \bar{\phi}_1(j) \cdot \bar{\phi}_2(j')$, with $J_{jj'}^2$ being a random coefficient whose configurational average vanishes. If $\bar{\phi}_1$ and $\bar{\phi}_2$ were components of a rotationally invariant $2m$ -component spin vector $(\bar{\phi}_1, \bar{\phi}_2)$, then it has recently been shown by one of us⁴⁰ that such random off-diagonal exchange terms would eliminate the possibility of having FM (or AFM) long-range order for $d < 4$. The reason for this is associated with the fact that in such systems, ordering of $\bar{\phi}_1$ with average \bar{M} yields an effective random magnetic field $\sum_j J_{jj'}^2 \bar{M}$ acting on $\bar{\phi}_2$, leading to a breakdown of long-range order in $\bar{\phi}_2$. The system simply prefers to break into domains in which $\bar{\phi}_2$ follows the local random field.⁴¹

In fact, $\bar{\phi}_1$ and $\bar{\phi}_2$ do not correspond to components of a rotationally invariant vector, and this may make the arguments given above irrelevant. In some cases, the effect of symmetry-breaking terms was shown to turn the transition *first order*.⁴⁰

(iv) *Spin-glass ordering.* The argument involving an effective random field, mentioned above, is already indicative that the spins in the system may sometimes prefer to freeze in random directions, i.e., form a spin-glass phase.⁴⁰ Indeed, the spin glass was invented exactly for systems in which both FM and AFM exchange interactions occur.¹⁹ Mean-field theory for such systems yields a spin-glass phase separating the FM and the AFM phases.¹⁹ These results have also been confirmed using the renormali-

zation group at $d = 6 - \epsilon$.^{19(e)} It turns out, that a spin-glass phase will not separate between FM and AFM phases if $\Delta J^2 < C [J]_{\text{av}}^2$, where $[J]_{\text{av}}$ and ΔJ^2 are the couplings average and variance respectively and C is a constant of order unity, depending on the lattice. As we pointed out in the end of Sec. III, one has $[J]_{\text{av}} = 0$ at the multicritical point when only nearest-neighbor interactions are present in a FM-AFM alloy. One should therefore expect a spin glass separating the FM and AFM phases in this case. In order to obtain a phase diagram with the FM and AFM phases meeting at a point, of the kind studied in the present paper, one should include at least next-nearest-neighbor interactions. In those cases, the phase diagrams of Fig. 1 are rediscovered. Analysis of these situations at $d = 6 - \epsilon$, will be given separately.²⁰

At this stage, we have no reason to rule out any of the possibilities listed above. Unfortunately, none of the existing experiments, some of which we review below, approach *the close vicinity of the multicritical point*. The effects described above result from *critical fluctuations*, and therefore such a close approach is necessary in order to check them. Farther away from the multicritical point (and from the critical lines) *mean-field theory* is sufficient. As we shall see, all the experiments indeed verify mean-field predictions where these apply. In particular, experiments confirm the nature of the ordered phases. All the experiments find a mixed phase, i.e., Fig. 1(a),⁵⁻⁹ with perpendicular magnetization and staggered magnetization when $m > 1$.

In our mean-field calculation we studied the conditions for various space-averaged long-range magnetic orderings to occur. We did not study the possibility that different types of ions will exhibit different types of ordering. For *bond* randomness, all the magnetic ions are identical and the space-averaged order parameters $\bar{\phi}_k$ are indeed the most general order parameters appropriate for the description of long-range magnetic ordering. For *site* random alloys there are different types of magnetic ions, say A and B , which form the alloy. In this case one can define order parameters describing long-range magnetic orderings for which the A and B ions order in different ways.^{7(a),42} The space-averaged order parameters $\bar{\phi}_k$ are not sensitive to such differences. A calculation performed in the Bethe-Peierls approximation, for an alloy obtained by mixing an Ising FM (A ions) with an Ising AFM (B ions), shows that the following ordered phases are obtained: (a) FM—all ions order ferromagnetically, (b) AFM—the two types of ions order antiferromagnetically with respect to ions of the same type, (c) if J_{AB} , the coupling between A and B ions, is sufficiently small there exists a mixed phase in which the A ions order ferromagnetically and the B ions order antiferromagnetically. Our space-averaged order parameters $\bar{\phi}_k$ are combinations of these order

parameters. Further calculations are required to determine whether the order parameters of Refs. 7(a) and 42, the $\bar{\phi}_k$, or maybe combinations of these are appropriate for the description of the ordered phases of random alloys. Experimental data indicate that for the random-site Ising magnet^{7(b)} there are no distinct orderings of the A and B ions although this aspect of the results is not definite. We assumed that the $\bar{\phi}_k$ are the appropriate order parameters for the description of the magnetic orderings in the random alloy. We believe that the possible modifications due to possible different orderings of the A and B ions in the random-site alloy are irrelevant for critical properties when magnetic long-range order exists, since (as was already pointed out) a random-site alloy can be regarded as a random-bond alloy with short-range correlations which become unimportant in the critical region.¹⁸

In addition to all these comments, we emphasize that all the theoretical and experimental limitations of I (Sec. IV there) apply also here and will not be repeated.

Finally, we discuss some experiments. In most of the experimental data the phase diagrams are incomplete, since any change of the concentration requires growing a new crystal. It seems that most of the experiments were performed mainly to determine the nature of the ordered phases. We recommend to repeat them in order to study the *critical* properties predicted in this work.

We review the following experiments.

(i) $\text{Fe}(\text{Pd}_p\text{Pt}_{1-p})_3$.⁵ FePd_3 is a Heisenberg ($m = 3$) FM and FePt_3 is a Heisenberg AFM. The main contribution to the magnetization is due to magnetic moments of the Fe ions, and therefore this is an example of a random-bond alloy. The resulting phase diagram is that depicted in Fig. 1(a), where I and II denote FM and AFM. The mixed phase has canted magnetic moments with the FM order parameter perpendicular to the AFM order parameter in agreement with the predictions of Sec. III. The transition between the AFM and the mixed phase is first order. In the mean-field approximation, the free energy per degree of freedom reduces to that of a pure system (Sec. III). Recent numerical mean-field calculations on pure systems⁴³ (avoiding the Landau expansion performed in this work) show that the second-order transition lines between the mixed phase and the one component, ordered phases (corresponding to T_1' and T_2' of Fig. 1(a) in the present work) may turn first order sufficiently below the tetracritical point. This argument may be the explanation for the first-order transition between the AFM and mixed phases.

(ii) $\text{Fe}_p\text{Ni}_{1-p}$.⁶ We are aware of data only for $p = 0.63$ (in addition to $p = 1$ or $p = 0$, of course), where a canted magnetic structure was observed with the staggered magnetization perpendicular to the magnetization.

(iii) $(\text{Fe}_p\text{Mn}_{1-p})\text{WO}_4$,⁷ FeWO_4 and MnWO_4 are AFM's with different periodicities. Since the magnetization is due to Fe and Mn moments, this is a random-site alloy. The spins tend to align in a preferred direction, and therefore these are examples of Ising AFM's. The phase diagram shows a mixed phase, where both types of orderings coexist. It seems^{7(e)} that there are no distinct orderings of the Fe and Mn ions, in contradiction to Refs. 7(a) and 42.

(iv) $(\text{Mn}_{1-p}\text{Cr}_p)\text{Sb}$.⁸ MnSb is an X - Y ($m=2$) FM with the magnetization perpendicular to the c axis. CrSb is an Ising ($m=1$) AFM with the staggered magnetization in the c direction. $(\text{Mn}_{1-p}\text{Cr}_p)\text{Sb}$ is a random-site alloy, exhibiting the phase diagram schematically depicted in Fig. 3. (Not all the boundaries between the phases were determined by experiments; only the existence of various ordered phases was determined by experiments.) The ordered phases are as follows: (a) FM, ordering perpendicular to the c axis, corresponding to pure MnSb ordering; (c) AFM ordering perpendicular to the c axis; (b) coexistence of FM and AFM orderings perpendicular to each other and perpendicular to the c axis (canted phase); (e) AFM ordering parallel to the c axis, corresponding to pure CrSb ordering; (d) coexistence of AFM orderings parallel and perpendicular to the c axis. At the multicritical point B of Fig. 3 two phases in which different components of the same order-parameter order. This is exactly the point studied in I. The multicritical point A is the type studied in the present paper. The complete understanding of the phase diagram of this alloy will shed light on the nature of the critical behavior of random alloys, and especially on multicritical behavior. Therefore experimental determination of all the phase boundaries is worthwhile.

(v) $\text{Tb}(\text{Cu}_{1-p}\text{Zn}_p)$.⁹ Pure TbCu is AFM and pure TbZn is Fm. $\text{Tb}(\text{Cu}_{1-p}\text{Zn}_p)$ is a random-bond alloy, exhibiting a canted mixed phase. The special property of this alloy is the direct transition from the mixed phase to the paramagnetic phase, extending along a

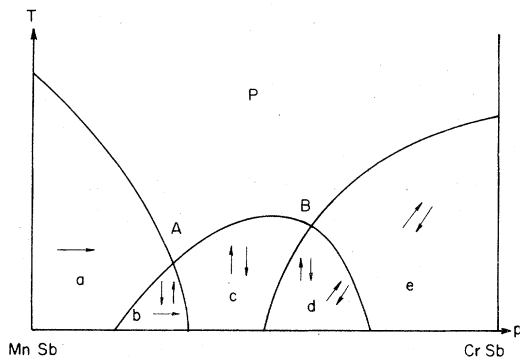


FIG. 3. Schematic phase diagram of $(\text{Mn}_{1-p}\text{Cr}_p)\text{Sb}$ (see text).

finite range of concentrations. This transition cannot be of the usual second-order nature. To see this, assume that the transition is second order. At a transition point from the paramagnetic to the mixed phase both $\vec{\phi}_1$ and $\vec{\phi}_2$ become ordered. In mean-field theory such a transition point has $r_1(p, T) = 0$ and $r_2(p, T) = 0$. Since $\vec{\phi}_1$ and $\vec{\phi}_2$ exhibit different symmetry properties, r_1 and r_2 vanish simultaneously only at a single point in the p - T plane. Therefore, this transition is either smeared or first order, a possibility mentioned in the end of Sec. II. Alternatively, it may consist of several transitions which were not separated experimentally, forming a phase diagram of the type of Fig. 3. It also seems that the mixed phase splits into different phases, since at different points in this phase a different order parameter was measured. More measurements in the mixed phase are required to understand this phase diagram.

(vi) Phase diagrams similar to the last two examples may occur for $\text{Tb}(\text{Ag}_p\text{In}_{1-p})$,¹⁰ and for $\text{Gd}(\text{Ag}_p\text{In}_{1-p})$.¹¹ The phase diagrams (iv)–(vi) are affected by the presence of mobile electrons and holes.⁴⁴ This effect was not taken into account in our model, and it may turn to be important for the determination of the phase diagrams.

(vii) $\text{U}(\text{As}_p\text{Se}_{1-p})$,¹² $\text{U}(\text{P}_{1-p}\text{S}_p)$.¹³ The phase diagrams here are very complicated, exhibiting many different phases. This is probably due to interactions which were not taken into account in our model.

Although all the experiments described above confirm the general mean-field predictions, especially concerning the nature of the ordered phases, many more experiments are needed in order to check our more detailed predictions in the critical region. Of special interest in this context are the following questions: (a) Is the transition at the multicritical-point first order? (b) Is there a direct transition from the paramagnetic to the mixed phase along a line or is there some intermediate ordering between them? If there is, what is the nature of this ordering? (c) Is there a spin-glass ordering in the vicinity of the multicritical point? In addition to these questions, experimental information on critical exponents near the various critical lines and multicritical points will also be quite helpful.

Different answers may probably be expected for different systems. These will enable one to identify additional parameters which are important in determining the critical properties of random systems. This may help in constructing a more coherent theory of critical phenomena in random systems.

ACKNOWLEDGMENT

This research was supported by a grant from the United States–Israel Binational Science Foundation (BSF), Jerusalem, Israel.

- ¹For a recent review, see, e.g., A. Aharony, J. Magn. Magn. Mater. **7**, 198 (1978).
- ²S. Fishman and A. Aharony, Phys. Rev. B **18**, 3507 (1978). This paper is referred to as I in what follows. A. Aharony and S. Fishman, Phys. Rev. Lett. **37**, 1587 (1976).
- ³M. E. Fisher and D. R. Nelson, Phys. Rev. Lett. **32**, 1350 (1974); D. R. Nelson, J. M. Kosterlitz, and M. E. Fisher, *ibid.* **33**, 813 (1974); J. M. Kosterlitz, D. R. Nelson, and M. E. Fisher, Phys. Rev. B **13**, 412 (1976); M. E. Fisher, AIP Conf. Proc. **24**, 273 (1975); M. E. Fisher and D. R. Nelson, Phys. Rev. B **12**, 263 (1975).
- ⁴A. Aharony and D. Bruce, Phys. Rev. Lett. **33**, 427 (1974); A. Aharony, K. A. Müller, and W. Berlinger, *ibid.* **38**, 33 (1977); A. D. Bruce and A. Aharony, Phys. Rev. B **11**, 478 (1975); A. Aharony, in Proceedings of the 13th IUPAP Conference on Statistical Physics, Haifa, 1977; Ann. Israel Phys. Soc. **2**, 13 (1978).
- ⁵V. V. Kelarev, S. K. Sidorov, V. V. Klyushin, and R. Z. Abdulov, Phys. Status Solidi **24**, 385 (1967); J. S. Kouvel and J. B. Forsyth, J. Appl. Phys. **40**, 1359 (1969); J. Pebler, F. W. Richter, and E. Vogt, Phys. Status Solidi A **11**, 101 (1972); Ch. Wissel, Phys. Status Solidi B **51**, 669 (1972).
- ⁶S. F. Dubinin, S. K. Sidorov, S. G. Teploukhov, and V. E. Arkhipov, Pis'ma Zh. Eksp. Teor. Fiz. **18**, 550 (1973) [JETP Lett. **18**, 324 (1973)].
- ⁷(a) F. Wegner, Solid State Commun. **12**, 785 (1973); (b) Ch. Klein, *ibid.* **12**, 773 (1973); (c) H. Dachs, H. Weitzel and E. Stoll, *ibid.* **4**, 473 (1966); (d) H. Dachs, *ibid.* **7**, 1015 (1969); (e) H. Weitzel, *ibid.* **7**, 1249 (1969); (f) H. A. Obermayer, H. Dachs and H. Schröcke, *ibid.* **12**, 779 (1973); (g) R. Geller, Ch. Klein and K. Knorr, J. Magn. Magn. Mater. **4**, 199 (1977).
- ⁸(a) W. J. Takei, D. E. Cox, and G. Shirane, Phys. Rev. **129**, 2008 (1963); (b) M. Pasternak and P. Vernes, Solid State Commun. **15**, 1189 (1974).
- ⁹T. Yeshiro, Y. Hamaguchi, and H. Watanabe, J. Phys. Soc. Jpn. **40**, 64 (1976).
- ¹⁰J. W. Cable, W. C. Koehler, and H. R. Child, J. Appl. Phys. **36**, 1096 (1965).
- ¹¹K. Sekizawa and K. Yasukochi, Phys. Lett. **11**, 216 (1964).
- ¹²J. Leciejewicz, R. Tróc, A. Muresik, and T. Palewski, Phys. Status Solidi B **48**, 445 (1971).
- ¹³M. Kuznietz, G. H. Lander, and Y. Baskin, J. Appl. Phys. **40**, 1130 (1969); G. H. Lander, N. Kuznietz, and D. E. Cox, Phys. Rev. **188**, 963 (1969).
- ¹⁴D. Mukamel and S. Krinsky, Phys. Rev. B **13**, 5065 (1976); **13**, 5078 (1976); P. Bak and D. Mukamel, *ibid.* **13**, 5086 (1976).
- ¹⁵S. A. Brazovskii, I. E. Dzyaloshinskii, and B. G. Kuzharenko, Zh. Eksp. Teor. Fiz. **70**, 2257 (1969) [Sov. Phys. JETP **43**, 1178 (1976)].
- ¹⁶A. Aharony, Y. Imry, and S.-K. Ma, Phys. Rev. B **13**, 466 (1976).
- ¹⁷P. Bak, Phys. Rev. B **14**, 3980 (1976).
- ¹⁸A. B. Harris and T. C. Lubensky, Phys. Rev. Lett. **33**, 1540 (1974); T. C. Lubensky, Phys. Rev. B **11**, 3573 (1975).
- ¹⁹(a) D. Sherrington, AIP Conf. Proc. **29**, 224 (1975); (b) S. F. Edwards and P. W. Anderson, J. Phys. F **5**, 965 (1975); (c) D. Sherrington and S. Kirkpatrick, Phys. Rev. Lett. **35**, 1792 (1975); (d) S. Kirkpatrick and D. Sherrington, Phys. Rev. B **17**, 4384 (1978); (e) J. H. Chen and T. C. Lubensky, Phys. Rev. B **16**, 2106 (1977).
- ²⁰S. Fishman and A. Aharony (unpublished).
- ²¹D. C. Mattis, Phys. Lett. **56A**, 421 (1976); A. Aharony and Y. Imry, Solid State Commun. **20**, 899 (1976); J. M. Luttinger, Phys. Rev. Lett. **37**, 778 (1976); A. B. Harris and T. C. Lubensky, Phys. Rev. B **16**, 2141 (1977).
- ²²G. Grinstein, Ph.D. thesis (Harvard University, 1974) (unpublished); G. Grinstein and A. H. Luther, Phys. Rev. B **13**, 1329 (1976).
- ²³V. J. Emery, Phys. Rev. B **11**, 239 (1975).
- ²⁴K. G. Wilson and J. Kogut, Phys. Rep. **12**, 75 (1974).
- ²⁵S.-K. Ma, *Modern Theory of Critical Phenomena* (Benjamin, Reading, Mass., 1976).
- ²⁶A. Aharony, in *Phase Transitions and Critical Phenomena*, edited by C. Domb and M. S. Green (Academic, New York, 1976), Vol. 6, p. 357.
- ²⁷D. E. Khmel'nitzkii, Zh. Eksp. Teor. Fiz. **68**, 1960 (1975) [Sov. Phys. JETP **41**, 981 (1976)]; see also A. Aharony, Phys. Rev. B **13**, 2092 (1976).
- ²⁸A. B. Harris, J. Phys. C **7**, 1671 (1974).
- ²⁹A. Aharony, Phys. Rev. Lett. **34**, 590 (1975). This letter analyzed the consequences of approaching the "isotropic $n \rightarrow 0$ " fixed point, which we now believe cannot be approached.
- ³⁰S. Krinsky and D. Mukamel, Phys. Rev. B **16**, 2313 (1977).
- ³¹J. Hubbard, Phys. Lett. **39A**, 365 (1972).
- ³²E. Domany, D. Mukamel, and M. E. Fisher, Phys. Rev. B **15**, 5432 (1977).
- ³³D. Mukamel, presented at the Annual Meeting of the Israel Physical Society, April, 1978 (unpublished).
- ³⁴K.-S. Liu and M. E. Fisher, J. Low Temp. Phys. **10**, 655 (1972).
- ³⁵A. D. Bruce, M. Droz, and A. Aharony, J. Phys. C **7**, 3673 (1974).
- ³⁶A. Aharony, Phys. Rev. B **12**, 1038 (1975).
- ³⁷M. E. Fisher and P. Pfeuty, Phys. Rev. B **6**, 1889 (1972); F. J. Wegner, *ibid.* **1891** (1972); P. Pfeuty, D. Jasnow, and M. E. Fisher, *ibid.* **10**, 2088 (1974).
- ³⁸A. Aharony, Phys. Lett. **59A**, 163 (1976).
- ³⁹D. J. Thouless, P. W. Anderson, and R. G. Palmer, Philos. Mag. **35**, 593 (1977).
- ⁴⁰A. Aharony, Solid State Commun. (to be published).
- ⁴¹Y. Imry and S.-K. Ma, Phys. Rev. Lett. **35**, 1399 (1975).
- ⁴²E. Eggarter and T. P. Eggarter, Phys. Rev. B **15**, 2804 (1977).
- ⁴³M. Kerszberg and D. Mukamel, Phys. Rev. B **18**, 6283 (1978).
- ⁴⁴P. G. de Gennes, Phys. Rev. **118**, 141 (1960).